



Return of Collective Rotation in ^{157}Er and ^{158}Er at Ultrahigh Spin

E. S. Paul,¹ P. J. Twin,¹ A. O. Evans,¹ A. Pipidis,² M. A. Riley,² J. Simpson,³ D. E. Appelbe,³ D. B. Campbell,^{2,*} P. T. W. Choy,¹ R. M. Clark,⁴ M. Cromaz,⁴ P. Fallon,⁴ A. Görgen,^{4,†} D. T. Joss,^{3,‡} I. Y. Lee,⁴ A. O. Macchiavelli,⁴ P. J. Nolan,¹ D. Ward,⁴ and I. Ragnarsson⁵

¹Oliver Lodge Laboratory, University of Liverpool, Liverpool L69 7ZE, United Kingdom

²Department of Physics, Florida State University, Tallahassee, Florida 32306, USA

³CCLRC Daresbury Laboratory, Daresbury, Warrington WA4 4AD, United Kingdom

⁴Nuclear Science Division, Lawrence Berkeley National Laboratory, Berkeley, California 94720, USA

⁵Department of Mathematical Physics, Lund Institute of Technology, P.O. Box 118, S-22100 Lund, Sweden

(Received 5 September 2006; published 5 January 2007)

A new frontier of discrete-line γ -ray spectroscopy at ultrahigh spin has been opened in the rare-earth nuclei $^{157,158}\text{Er}$. Four rotational structures, displaying high moments of inertia, have been identified, which extend up to spin $\sim 65\hbar$ and bypass the band-terminating states in these nuclei which occur at $\sim 45\hbar$. Cranked Nilsson-Strutinsky calculations suggest that these structures arise from well-deformed triaxial configurations that lie in a valley of favored shell energy which also includes the triaxial strongly deformed bands in $^{161-167}\text{Lu}$.

DOI: 10.1103/PhysRevLett.98.012501

PACS numbers: 21.10.Re, 23.20.En, 23.20.Lv, 27.70.+q

The response of atomic nuclei to increasing angular-momentum values, or rotational stress, continues to be a fundamental and fascinating field of scientific study. Indeed, the quest to observe ever increasing high-spin states in nuclei has driven the field of γ -ray nuclear spectroscopy for many decades. In the rare-earth region of the nuclear landscape, nuclei can accommodate the highest values of angular momentum and have provided a wealth of new nuclear-structure phenomena. Some central topics include the spectroscopy of (i) superdeformed (SD) nuclei around ^{152}Dy [1], (ii) triaxial strongly deformed (TSD) bands and the associated “wobbling” motion in nuclei around ^{163}Lu [2], (iii) highly deformed structures in $A \sim 174$ Hf nuclei [3,4], and (iv) band termination in $N \sim 90$ nuclei [5–9].

In this Letter, the identification of very weakly populated rotational bands in the $N \sim 90$ nuclei $^{157,158}\text{Er}$, with high moments of inertia, is reported. These structures bypass the terminating configurations, marking a return to collectivity that extends discrete γ -ray spectroscopy to well over $60\hbar$ in these nuclei. State-of-the-art cranking calculations suggest that these structures may represent triaxial strongly deformed bands that lie in a valley of favored shell energy in deformation and particle-number space.

The $^{157,158}\text{Er}$ isotopes have featured prominently as the spectroscopy of nuclei at extreme spin has progressed. A schematic diagram of the structural evolution with spin in the nucleus ^{158}Er is shown in Fig. 1, where the interplay of numerous coexisting structures near the yrast line is illustrated. ^{158}Er was one of the initial nuclei in which Coriolis-induced pair breaking (backbending) was discovered [10] and the first nucleus in which the second alignment was observed [11]. In Fig. 1, the first alignment of two $i_{13/2}$ neutrons at spin $\sim 14\hbar$ is indicated, together with the

second alignment of two $h_{11/2}$ protons at spin $\sim 28\hbar$. At spin $38\hbar$, a dramatic change of structure occurs along the yrast line when less-collective band structures become energetically favored [6,12]. These bands reach high spin by aligning their valence single-particle angular momenta, outside the $^{146}\text{Gd}_{82}$ doubly magic core, causing the shape of the nucleus to become oblate. The bands then terminate at the maximum value of spin available to the valence particles. In ^{158}Er , band termination occurs at spin

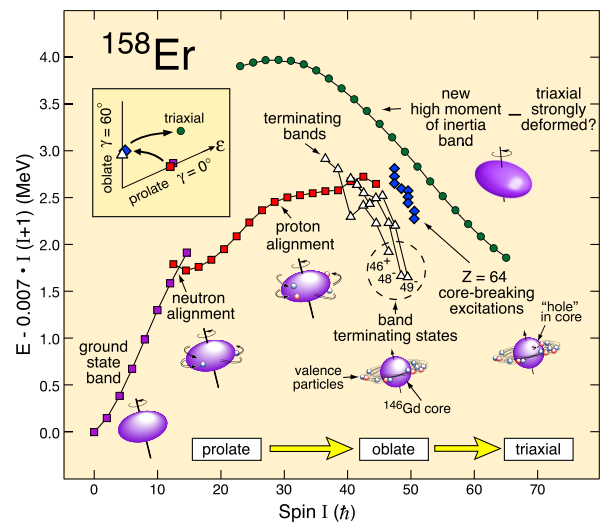


FIG. 1 (color online). Evolution of the nuclear structure of ^{158}Er with spin. Excitation energies of a variety of observed structures are plotted with respect to a rigid-rotor reference in order to emphasize the changes that occur along and close to the yrast line. The strongest new high moment-of-inertia band is included, but its exact excitation energy is not known. The inset illustrates the changing shape of ^{158}Er with increasing spin within the standard (ϵ, γ) deformation plane.

46–49 \hbar when all of the 12 valence-particle spins are maximally aligned in specific nucleonic configurations. Indeed, this nucleus provides the textbook example of the phenomenon of band termination in heavy nuclei [13,14].

In order to generate further angular momentum, the proton $Z = 64$ core (in $^{146}\text{Gd}_{82}$) has to be broken, which costs about 1 MeV of energy at 50 \hbar (see Fig. 1). It has been a goal for many years to establish the nature of the yrast states in these nuclei in the spin range from 50 to 70 \hbar , well beyond the very favored band-termination states. Recently, we have observed a multitude of weak high-energy γ rays feeding into the band-terminating states of ^{157}Er [15] and, to a lesser extent, ^{156}Er and ^{158}Er [16]. The structure of these states is consistent with a single-particle, oblate interpretation and, with the help of cranking-model calculations, specific configurations involving core breaking could be identified [15]. These new states only advanced discrete γ -ray spectroscopy by a further one or two units of spin, and the puzzle of the missing spin regime from 50 \hbar to fission remained. However, the newly identified structures now extend discrete levels in $^{157,158}\text{Er}$ to beyond 60 \hbar .

In order to populate the ultrahigh-spin states in $^{157,158}\text{Er}$, a 215 MeV ^{48}Ca beam, provided by the 88 Inch Cyclotron accelerator at the Lawrence Berkeley National Laboratory, was used to bombard two stacked thin self-supporting foils of ^{114}Cd of total thickness 1.1 mg/cm 2 . A total of 1.2×10^9 events were collected using the Gammasphere spectrometer [17], when at least seven of the 102 Compton-suppressed HPGe detectors fired in prompt coincidence. In the off-line analysis, approximately 6.5×10^{10} quadruples (γ^4) were unfolded from the data set and replayed into a Radware-format [18] four-dimensional hypercube for γ -ray coincidence analysis. A search for rotational bands with relatively high moments of inertia was performed in the hypercube which resulted in the identification of four sequences, with two in ^{158}Er and two in ^{157}Er . Improved spectra were then obtained from the raw data by analysis of high-fold events (at least sevenfold, γ^7) by setting multiple ($n \leq 5$) coincidence gates to produce 1D spectra using the “spikeless” method [19]. The transition energies in the new bands are listed in Table I, and coincident γ -ray spectra for the two strongest structures (labeled band 1 in Table I) are shown in Fig. 2. These bands are estimated to carry only $\sim 10^{-4}$ of the respective channel intensity, i.e., 2 orders of magnitude lower than the yrast SD band in ^{152}Dy [1]. The two other bands in $^{157,158}\text{Er}$ (labeled band 2 in Table I) are a factor of 2–3 lower in intensity. A high-fold analysis of the intensity profiles at the bottom of band 1 in ^{158}Er , in comparison to feeding intensities into the known yrast states with parity (π) and signature (α) [9] given by $(\pi, \alpha) = (+, 0)$, $(-, 1)$, and $(-, 0)$ (see Fig. 2), allowed an estimation of the highest spin reached by this band of $\sim 65\hbar$. In ^{157}Er , band 1 rapidly depopulates over one transition and is estimated to extend up to $\sim 60\hbar$.

TABLE I. Gamma-ray energies of the new high-spin bands in $^{157,158}\text{Er}$. The energies are accurate to ± 0.5 keV, except those values quoted as integers, which are accurate to ± 1 keV.

^{158}Er			^{157}Er		
Band 1	Band 2		Band 1	Band 2	
724.3	1156.3	959	778.5	1311.5	956
766.6	1204.9	1007	805.5	1372.2	998
802.3	1255.9	1046	850.5	1435.6	1044
841.7	1310.2	1083	905.1	1501	1093
875.0	1369.0	1124	955.9	1572	1138
901.5	1430.2	1167	1005.4		1186
932.6	1491	1212	1053.7		1236
972.7	1562	1260	1101.0		1287
1017.6	1625	1309	1150.5		1345
1064.3	1702	1360	1201.0		1402
1110.1		1416	1254.2		1464

The high moment-of-inertia values of the new band 1 sequences in $^{157,158}\text{Er}$ are illustrated in Fig. 3 and compared with other strongly deformed bands in the region. The moment-of-inertia trajectories for the weaker band 2 sequences in $^{157,158}\text{Er}$ show similar trends.

In order to interpret the new high-spin sequences in $^{157,158}\text{Er}$, calculations have been performed in the framework of the configuration-dependent, cranked Nilsson-Strutinsky formalism without pairing [9,20]. The yrast states in the $I = 50$ –60 spin range are built from terminating bands, but a series of collective configurations is predicted at a relatively small excitation energy [5,21]. These involve shape-driving high- j proton $i_{13/2}$ and/or $h_{9/2}$ orbitals, which are common ingredients of high-spin high-deformation structures throughout the rare-earth region. The special feature distinguishing these configurations from less-collective ones is, however, the presence of neutron holes in upsloping orbitals which originate from subshells below the $N = 82$ shell closure.

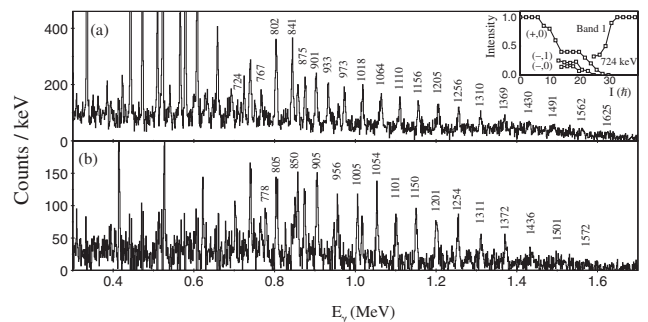


FIG. 2. Background-subtracted coincident γ^5 spectra illustrating the two strongest sequences observed in (a) ^{158}Er and (b) ^{157}Er . The strong unlabeled peaks represent the low-spin yrast structures in these nuclei. The relative intensity profiles of the new (band 1) sequence in ^{158}Er and known structures around the feedout region are shown in the inset in (a).

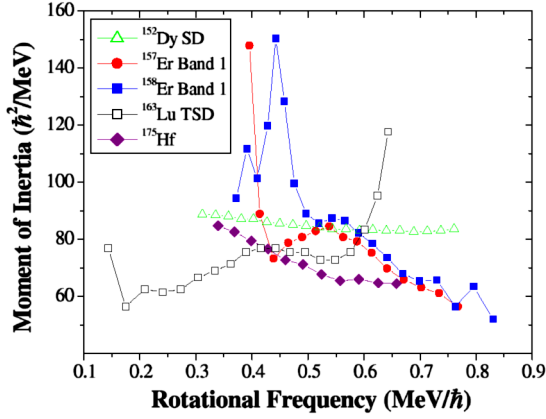


FIG. 3 (color online). Dynamic moments of inertia as a function of rotational frequency for the new (band 1) sequences in $^{157,158}\text{Er}$, the yrast SD band in ^{152}Dy [1], a TSD band in ^{163}Lu [2], and the strongly deformed band in ^{175}Hf [4].

The variation of shell energy as a function of particle number and deformation is a decisive factor concerning which nuclear shapes are realized. Long ago, it was observed that, if the calculated shell energy is plotted as a function of particle number and quadrupole deformation, valleys of favored energy will intersect this landscape in such a way that increasing particle number leads to increasing deformation [22]. It is now well established, see, e.g., Ref. [23], and references therein, that the evolution of deformations for the superdeformed bands in the $A = 140\text{--}150$ region can be understood from such a valley (cf. Ref. [24]) and that this valley can be followed from ^{152}Dy to ^{132}Ce [25], as illustrated in Fig. 4, and even down to the smooth terminating bands in the $A = 110$ region [26]. A common feature of the configurations in this valley is the presence of two proton holes in the upsloping $[404]9/2$ orbital, emerging from the $g_{9/2}$ shell located below the spherical $Z = 50$ closure.

An analogous shell-energy valley can be defined for configurations with two neutron holes in the upsloping $[505]11/2$ orbital, emerging from the $h_{11/2}$ shell located below the spherical $N = 82$ gap. This valley, shown by the dashed line in Fig. 4(a), is, however, not so well developed, but collective bands in ^{154}Dy [27] (and possibly ^{152}Dy [28]) can be seen as a manifestation of this valley. Furthermore, if the observed highest-spin band in ^{175}Hf [3] is assumed to belong to this valley, i.e., with a configuration with two $h_{11/2}$ holes, the calculated quadrupole moment comes close to experiment.

However, as illustrated in Fig. 4(b), a new valley opens for nonaxial deformations with $\gamma \approx 20^\circ$. This is because of the coupling within the upsloping equatorial $N_{\text{osc}} = 4$, $n_z = 0$ orbitals, according to the mechanism discussed in Ref. [29]. This coupling causes the $[402]3/2$ and the $[400]1/2$ orbitals to split apart, and a region of low level density is formed in between. This valley is characterized by two neutron holes in the $[505]11/2$ orbital but, in

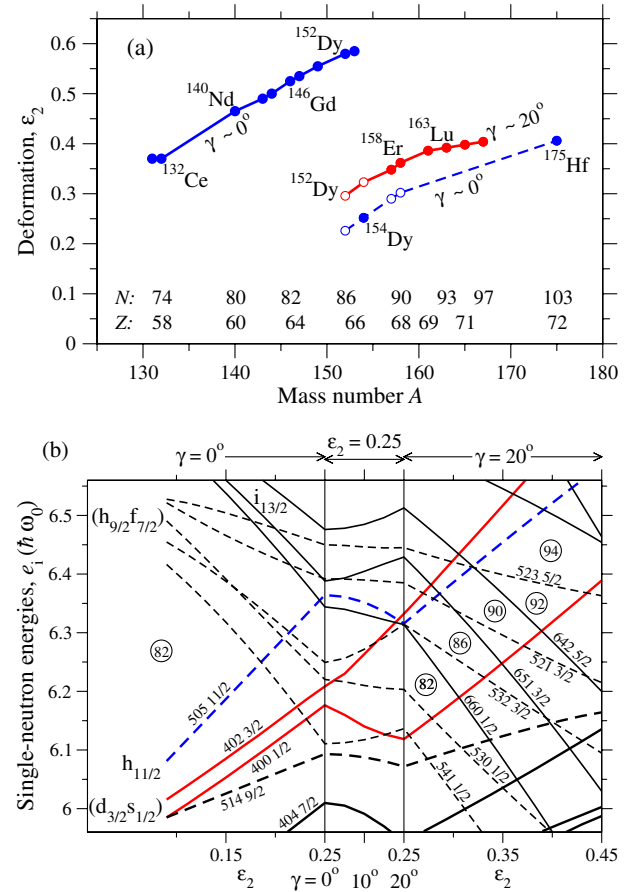


FIG. 4 (color online). (a) Calculated deformations for some well-deformed configurations. Axial ($\gamma = 0^\circ$) SD configurations involving proton holes in the $g_{9/2}$ $[404]9/2$ orbital are shown for nuclei from ^{132}Ce to ^{152}Dy . Similar axial deformations for configurations involving neutron holes in the $h_{11/2}$ $[505]11/2$ orbital are shown for nuclei from ^{152}Dy to ^{175}Hf . Triaxial ($\gamma \sim 20^\circ$) shapes are also predicted corresponding to a valley of low level density shown in (b) for neutron numbers $N = 82\text{--}94$. In (a), the solid data points indicate that corresponding experimental bands are established. In (b), single-neutron energies near $N = 90$ are shown as a function of deformation for $\gamma = 0^\circ$ in the left-hand panel. In the center panel, the elongation is kept constant with $\epsilon_2 = 0.25$, and γ is increased to 20° . The strong coupling within the upsloping $N_{\text{osc}} = 4$, $n_z = 0$ equatorial orbitals causes the $[402]3/2$ and $[400]1/2$ orbitals to split apart so that a region of low level density is created at $\gamma = 20^\circ$. This is illustrated in the right-hand panel where ϵ_2 is increased.

addition, two neutron holes in $N_{\text{osc}} = 4$ orbitals; see also Refs. [28,30]. The triaxial deformation in this valley is well established [31] in the Lu isotopes but appears to be as well developed in $^{157,158}\text{Er}$ and maybe also in $^{152,154}\text{Dy}$. Consequently, the most likely configuration for band 1 in ^{158}Er is $\pi[(g_{7/2}d_{5/2})^{-4}(h_{11/2})^6(h_{9/2})^1(i_{13/2})^1] \times \nu[(h_{11/2})^{-2}(N_{\text{osc}} = 4)^{-2}(h_{9/2}f_{7/2})^8(i_{13/2})^4]$, where the dominant components relative to a ^{146}Gd core are indicated. An alternative interpretation is that the high-spin bands in $^{157,158}\text{Er}$ are formed at close to axial shape [dashed

valley in Fig. 4(a)] with no neutron holes in the $N_{\text{osc}} = 4$ orbitals. The calculated minima for these two possibilities lie very close in excitation energy. However, the triaxial shape is the most likely interpretation since the potential energy minimum is much better developed. The new bands in $^{157,158}\text{Er}$ are then analogous to the TSD bands in the Lu isotopes.

In summary, four new band structures displaying high moments of inertia have been established in $^{157,158}\text{Er}$ to ultrahigh spin ($>60\hbar$). These sequences bypass and extend beyond the well-known band-terminating states in these nuclei ($\sim 45\hbar$). Comparison with cranked Nilsson-Strutinsky calculations suggests that these sequences are most likely strongly deformed ($\epsilon_2 = 0.30\text{--}0.35$) triaxial ($\gamma = 20^\circ\text{--}25^\circ$) structures. It is suggested that they have a common configuration component, involving two neutron holes in the $h_{11/2}$ [505]11/2 orbital and two neutron holes in the highest $N_{\text{osc}} = 4$ orbital. A valley of favored shell energy in deformation and particle-number space is formed below these orbitals at triaxial shape. It can be traced through collective bands in Dy nuclei, over the new bands in $^{157,158}\text{Er}$, to TSD bands in Lu nuclei.

This work was supported in part by the United Kingdom Engineering and Physical Sciences Research Council, the State of Florida, the National Science Foundation, the U.S. Department of Energy under Contract No. AC03-76SF00098, and the Swedish Science Research Council.

*Present address: Lawrence Livermore National Laboratory, Livermore, CA 94551, USA.

†Present address: DAPNIA/SPH N CEA Saclay, F-91191 Gif-sur-Yvette, France.

‡Present address: Oliver Lodge Laboratory, University of Liverpool, Liverpool L69 7ZE, United Kingdom.

[1] P. J. Twin *et al.*, Phys. Rev. Lett. **57**, 811 (1986).

[2] S. W. Odegard *et al.*, Phys. Rev. Lett. **86**, 5866 (2001).

[3] D. T. Scholes *et al.*, Phys. Rev. C **70**, 054314 (2004).

[4] D. J. Hartley *et al.*, Phys. Lett. B **608**, 31 (2005).

[5] T. Bengtsson and I. Ragnarsson, Phys. Scr. **T5**, 165 (1983).

[6] I. Ragnarsson, Z. Xing, T. Bengtsson, and M. A. Riley, Phys. Scr. **34**, 651 (1986).

[7] F. S. Stephens *et al.*, Phys. Rev. Lett. **54**, 2584 (1985).

[8] J. Simpson *et al.*, Phys. Lett. B **327**, 187 (1994).

[9] A. V. Afanasjev, D. B. Fossan, G. J. Lane, and I. Ragnarsson, Phys. Rep. **322**, 1 (1999).

[10] H. Beuscher *et al.*, Phys. Lett. **40B**, 449 (1972).

[11] I. Y. Lee *et al.*, Phys. Rev. Lett. **38**, 1454 (1977).

[12] J. Burde *et al.*, Phys. Rev. Lett. **48**, 530 (1982).

[13] K. Heyde, *Basic Ideas and Concepts in Nuclear Physics* (Institute of Physics, Bristol, 1999), p. 53.

[14] S. G. Nilsson and I. Ragnarsson, *Shapes and Shells in Nuclear Structure* (Cambridge University Press, Cambridge, England, 1995), p. 230.

[15] A. O. Evans *et al.*, Phys. Rev. Lett. **92**, 252502 (2004).

[16] M. A. Riley *et al.*, Phys. Scr. **T125**, 123 (2006).

[17] I. Y. Lee, Nucl. Phys. **A520**, c641 (1990).

[18] D. C. Radford, Nucl. Instrum. Methods Phys. Res., Sect. A **361**, 297 (1995).

[19] C. W. Beausang *et al.*, Nucl. Instrum. Methods Phys. Res., Sect. A **364**, 560 (1995).

[20] T. Bengtsson and I. Ragnarsson, Nucl. Phys. **A436**, 14 (1985).

[21] J. Dudek and W. Nazarewicz, Phys. Rev. C **31**, 298 (1985).

[22] I. Ragnarsson, S. G. Nilsson, and R. K. Sheline, Phys. Rep. **45**, 1 (1978).

[23] A. Neusser *et al.*, Phys. Rev. C **70**, 064315 (2004).

[24] J. Dudek, W. Nazarewicz, Z. Szymanski, and G. A. Leander, Phys. Rev. Lett. **59**, 1405 (1987).

[25] A. V. Afanasjev and I. Ragnarsson, Nucl. Phys. **A608**, 176 (1996).

[26] I. Ragnarsson, Acta Phys. Pol. B **27**, 33 (1996).

[27] W. C. Ma *et al.*, Phys. Rev. C **65**, 034312 (2002).

[28] D. E. Appelbe *et al.*, Phys. Rev. C **66**, 044305 (2002).

[29] S. E. Larsson, P. Möller, and S. G. Nilsson, Phys. Scr. **10A**, 53 (1974).

[30] H. Schnack-Petersen *et al.*, Nucl. Phys. **A594**, 175 (1995).

[31] G. B. Hagemann *et al.*, Eur. Phys. J. A **20**, 183 (2004).